

EPR studies of AsO_4^{4-} spin-lattice-relaxation times in antiferroelectric $\text{NH}_4\text{H}_2\text{AsO}_4$ and mixed glassy $\text{Rb}_{1-x}(\text{NH}_4)_x\text{H}_2\text{AsO}_4$ ($x = 0.35$)

S. Waplak,* Z. Trybula,* John E. Drumheller, and V. Hugo Schmidt

Physics Department, Montana State University, Bozeman, Montana 59717

(Received 21 May 1990)

The electron spin-lattice-relaxation time T_1 was measured for x-ray-induced AsO_4^{4-} centers in antiferroelectric $\text{NH}_4\text{H}_2\text{AsO}_4$ (ADA) and mixed $\text{Rb}_{1-x}(\text{NH}_4)_x\text{H}_2\text{AsO}_4$ (RADA, $x=0.35$) in the temperature range 4.2–300 K by the saturation method. It is shown that below T_0 $1/T_1$ reflects the direct relaxation process. From above T_0 to 55 K, $1/T_1 \propto T^{1.6}$ and can be described by a Vogel-Fulcher law $1/T_1 \sim (T - T_0)$. It is also shown that the flatness of $1/T_1$ in the temperature region from 55 to 120 K is due to the tunneling motion of nitrogen in the glassy phase of RADA. Contrary to ADA, the $1/T_1$ behavior in RADA reflects the fracton nature of relaxation in the spin-glass state.

I. INTRODUCTION

Systems with randomly competing interactions forming glasses upon lowering temperature are under active investigation.^{1–6} Dielectric measurements have recently shown⁷ the presence of glassy behavior in $\text{Rb}_{1-x}(\text{NH}_4)_x\text{H}_2\text{AsO}_4$ (RADA, $x = 0.35$). The proton spin relaxation and ^{87}Rb relaxation have been recently^{8,9} measured and described by a stretched-exponential relation. The most characteristic property¹⁰ of the glassy state is the dramatic change in the time scale of structural relaxation which reflects the extreme slowing down of the motional processes leading to atomic rearrangements. It is known that substitution of NH_4^+ for Rb in RbH_2AsO_4 changes the proton configurations from ferroelectric to antiferroelectric at low temperatures.¹¹ A wide spectrum of experimentally observed relaxation times for the similar proton glass $\text{Rb}_{1-x}(\text{NH}_4)_x\text{H}_2\text{PO}_4$ has been constructed^{12,13} from Raman, Brillouin, and dielectric measurements. However, each experimental technique deals with different quantities, since each technique is sensitive to those relaxation processes which are of the same order of magnitude as the characteristic measurement frequency.¹⁴ To get information about glass-state dynamics in the X-band region, we decided to measure the spin-lattice-relaxation time T_1 of the AsO_4^{4-} center formed after x irradiation in ADA ($\text{NH}_4\text{H}_2\text{AsO}_4$) and RADA in the wide temperature range from 4.2 to 300 K. To our knowledge such complete electron paramagnetic resonance (EPR) data for the proton glass state have not been obtained previously.

The AsO_4^{4-} center was chosen for two reasons: (a) the ferroelectric and antiferroelectric competition among proton-ordering arrangements taking place around each AsO_4 unit; and (b) the AsO_4^{4-} high-field hyperfine component (with hyperfine coupling $A \approx 1000$ G) is isolated both in ADA and RADA and therefore assures a high accuracy of relaxation measurements.

This paper is organized as follows: Sec. II gives a short explanation of the experimental conditions; Sec. III intro-

duces the equations used to analyze $1/T_1 = f(T)$; Sec. IV compares the results obtained for RADA and ADA; Sec. V summarizes the data and gives a possible description of $1/T_1$ versus temperature for relaxation in a fractal geometry in RADA.

II. EXPERIMENTAL

The pure ADA and mixed RADA crystals were grown by a method described elsewhere.^{7,15} Small-sized $2 \times 2 \times 4$ mm³ samples of ADA and RADA were next irradiated by an x-ray source with a copper anode operating at 20 kV and 10 mA for 6–8 h.

EPR measurements were made with a Varian X-band spectrometer operating with an Oxford liquid-helium system of temperature control and stabilization in the temperature range 4.2–300 K. The following paramagnetic centers, which decay after a few days, were detected by EPR: AsO_4^{4-} , AsO_3^{2-} , and NH_3^+ . Typical AsO_4^{4-} and AsO_3^{2-} spectra, well described by several authors,^{16–18} consist of two sets of quartets with high values of hyperfine constants, $A \approx 1000$ and 800 G which belong to AsO_4^{4-} and AsO_3^{2-} , respectively. In addition, lines of the NH_3^+ radical were observed in the central part of the spectra.¹⁵

At room temperature the AsO_4^{4-} spectrum can be derived from a spin Hamiltonian with the general form

$$\hat{H} = g\beta\hat{H}\hat{S} + \hat{S}\mathcal{A}^{\text{As}}\hat{I}_{\text{As}} + \hat{S}\mathcal{A}^{\text{H}}\hat{I}_{\text{H}}, \quad (1)$$

where g is the spectroscopic tensor, \hat{S} is the electron spin operator, \hat{I}_{As} , \hat{I}_{H} are the arsenic and proton nuclear spin operators, respectively, \mathcal{A}^{As} , \mathcal{A}^{H} are the tensors of hyperfine and superhyperfine structures, and β is the Bohr magneton.

The spin-Hamiltonian parameters for AsO_4^{4-} are listed in Table I. The last term of the Hamiltonian given by Eq. (1) gives only line broadening for the highest-field AsO_4^{4-} hyperfine component (unresolved superhyperfine proton structure). This line was single and symmetrical at 300 K down to 120 K, but line asymmetry was ob-

TABLE I. The spin-Hamiltonian parameters of the AsO_4^{4-} center at room temperature in RADA.

g_{iso}	1.998
$A_x(G)$	1025
$A_y(G)$	1026
$A_x(G)$	1138

served for large samples below 120 K and was reduced by minimizing sample size. This means that line asymmetry seen upon lowering temperature is due to the microwave electric-field component (electric dipole origin). The relaxation-time measurements for $\mathbf{a} \parallel \mathbf{H}_0$ have been done by the saturation method previously described by Poole,¹⁹ under the conditions discussed below.

III. SATURATION METHOD

The saturation theory for complex multilevel systems has been done by Lloyd and Pake²⁰ and expanded by Stephen and Frankel.²¹ These authors have shown²¹ that the saturation factor $S_{\alpha\beta}$ for multilevel systems may always be written in the form

$$S_{\alpha\beta} = (1 + 2V_{\alpha\beta}\Omega_{\alpha\beta})^{-1}, \quad (2)$$

where $V_{\alpha\beta}$ is the probability of the transition (α, β) induced by the radiation.

For a system with $S = \frac{1}{2}$, we have²¹

$$V_{\alpha\beta} = \frac{1}{4}\hbar^{-2}(g\beta)^2 H_{1s}^2 g_{\alpha\beta}(\gamma) D_{\alpha}, \quad (3)$$

where $g_{\alpha\beta}(\gamma)$ is the line-shape function, H_1 is the radiation field amplitude, and $D_{\alpha} = D(I, m_I)$ is the level degeneracy. The parameter $\Omega_{\alpha\beta}$ is related to what Lloyd and Pake²⁰ call the relaxation probability $(W_R)_{\alpha\beta}$ by

$$\Omega_{\alpha\beta} = [2(W_R)_{\alpha\beta}]^{-1}. \quad (4)$$

If a system consisting of an unpaired electron ($S = \frac{1}{2}$) interacting with a number of nuclei undergoes relaxation through mechanisms which are predominantly independent of the nuclear spin states, it effectively reduces to a set of two-level systems,²¹ and $D_{\alpha}\Omega_{\alpha\beta}$ takes the place of the spin-lattice-relaxation time T_1 appropriate for the description of saturation for a two-level spin system as used by Bloembergen, Purcell, and Pound.²²

In our case the line separation of hyperfine components of AsO_4^{4-} is very large (of order 1000 G) and the proton superhyperfine structure leads only to line broadening of the highest-field AsO_4^{4-} component, for which relaxation measurements are made. So, we can test our system as a predominantly two-level system for the $\frac{3}{2} \leftrightarrow \frac{3}{2}$ AsO_4^{4-} transition.

The simplest saturation theory for two-level systems was introduced by Bloembergen, Purcell, and Pound²² for homogeneously broadened Lorentzian lines. In our case the single EPR line of the highest-field AsO_4^{4-} hyperfine component should envelop an unresolved superhyperfine structure of protons around each AsO_4 tetrahedron, and the linewidth due to the distribution of superhyperfine

fields may be of the inhomogeneous type. For the low-field component a resolved superhyperfine structure is observed. Nevertheless, as has been shown by Portis,²³ if spin-spin relaxation time $T_2 \ll T_1$ (in our case $T_2 \approx 10^{-8}$ s, $T_1 \approx 10^{-4}$ s), the effect of inhomogeneity can be seen only in the reduction of the line intensity (compared with the homogeneous Lorentzian line) and in the appearance of a Gaussian line shape. The saturation coefficient at the center of a Gaussian line shape, when H_1 is adjusted to the value H_{1s} giving maximum line height, is

$$S(H_1 = H_{1s}) = (1 + \frac{1}{4}\gamma^2 H_{1s}^2 T_2 T_1)^{-1} = 0.5 \quad (4a)$$

with

$$T_2 = (2\pi)^{1/2} (\gamma \Delta H_{\text{pp}}^0)^{-1}, \quad (5)$$

where γ is the gyromagnetic ratio and ΔH_{pp}^0 is the first-derivative peak-to-peak linewidth below saturation. The relation between H_1^2 and the power values measured experimentally was taken from Varian manufacturer's data, which is given as²⁴

$$(H_1)_{\text{max}} = 1.475 \times 10^{-2} (QP)^{1/2}. \quad (6)$$

For the measured cavity Q of 2500 with sample and thermocouple in place, the relation between H_1^2 and P is

$$H_1^2 = 5.43 \times 10^{-4} P, \quad (7)$$

in mW, where P is in mW and H_1 is in G. Combining (4a), (5), and (7), the equation for T_1 becomes

$$T_1 = 1.81 \times 10^{-4} \frac{\Delta H_{\text{pp}}^0}{P_s}, \quad (8)$$

where ΔH_{pp}^0 is in G and P_s is the microwave power level in mW which assures saturation at a given T (see Fig. 2).

IV. EXPERIMENTAL RESULTS

The temperature dependence of linewidth ΔH_{pp}^0 for the highest-field component of AsO_4^{4-} in RADA is shown in Fig. 1. The linewidth reflects the expected random distribution of local fields²⁵ and can be fitted exactly by the equation

$$\Delta H_{\text{pp}}^0(T) = \Delta H_{\text{pp}}^{\text{ORT}} \left[1 + \tanh \frac{E_i}{kT} \right], \quad (9)$$

with $\Delta H_{\text{pp}}^{\text{RT}} = 15$ G and $E_i = 0.7$ meV (8.12 K), and the line shape is Gaussian in the temperature region under investigation.

To evaluate the temperature dependence of the spin-lattice-relaxation time T_1 , a set of saturation curves $Y_m = f(P)$ (Y_m being the first-derivative maximum amplitude) was made for each set of temperatures. Some saturation curves are presented in Fig. 2, and appear to be typical for homogeneously broadened lines.²⁶ The P_s power values assuring saturation are shown in Fig 3, where P_s is defined as the value giving maximum Y_m .

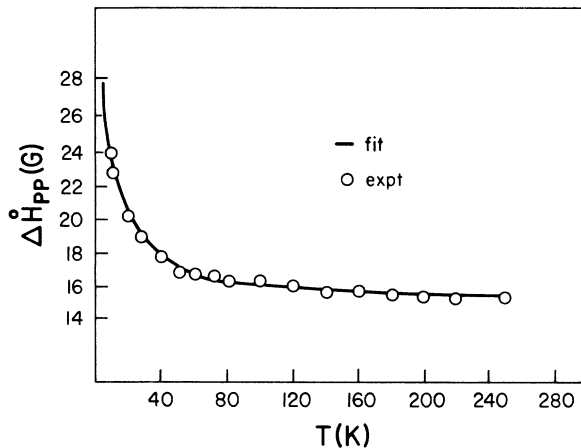


FIG. 1. The linewidth ΔH_{pp}^0 temperature evolution for the highest-field hyperfine component of AsO_4^{4-} in RADA.

Such a saturation behavior suggests, according to Eq. (8), that in some temperature regions (55–120 K) the spin-lattice-relaxation time T_1 in RADA is nearly temperature independent. This region is marked in Fig. 3 by the arrows. To check that it is a specific dependence for just the glassy state, we have compared the T_1 data for $x = 0.35$ RADA with the data for pure $x = 1$ ADA measured in the same way. The EPR line of AsO_4^{4-} (highest-field hyperfine component) is narrow ($\Delta H_{pp} \approx 6$ G) and with negligible temperature dependence of the linewidth (opposite to that of RADA, see Fig. 1). This line is accompanied by two symmetrically disposed satellite lines²⁷ with small intensities from “spin-flip” forbidden transitions. Up to about 45 K the main EPR line is not desaturated by spin flip (for $c \perp H_0$). This allows us to make a comparison of T_1 temperature dependences for ADA and RADA. The plots of $1/T_1 = f(T)$ for both RADA and ADA are presented in Fig. 4.

Before discussing the Fig. 4 data, two other experiments should be described below: (a) temperature dependence of the splitting of the AsO_4^{4-} highest-field line in

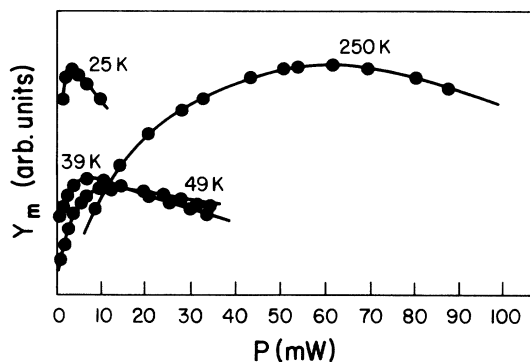


FIG. 2. Several saturation curves for the AsO_4^{4-} center in RADA.

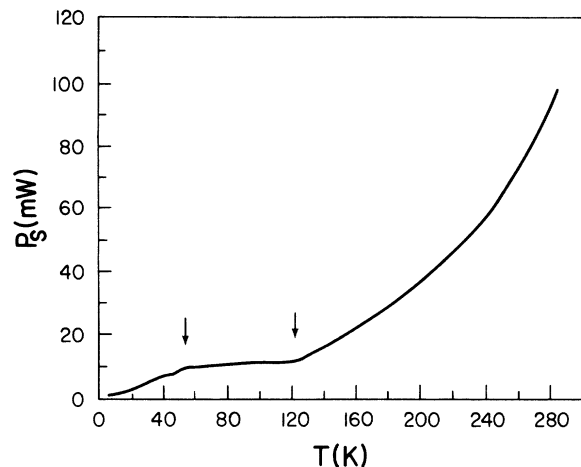


FIG. 3. The power values P_s assuring saturation conditions versus temperature for AsO_4^{4-} in RADA. The arrows indicate the limits of temperature-independent T_1 .

ferroelectric RbH_2AsO_4 (RDA), and (b) the behavior of the AsO_4^{4-} and NH_3^+ line intensities versus temperature for RADA.

Unlike the case for ADA, the AsO_4^{4-} line in RDA is evenly split [Fig. 5(a)] into four components below $T^* \approx 260$ K. The estimated correlation time τ_c for proton motion between Slater configurations for RDA evaluated from the line splitting shown in Figs. 5(a) and 5(b) is of order $\tau_c \geq \sqrt{2}/\gamma\Delta H = 4.5 \times 10^{-9}$ s. This means that in pure ADA this time is much shorter since there is no line splitting in the temperature range under investigation. For this reason and due to the random mixture of RDA and ADA, we can expect the presence of regions of

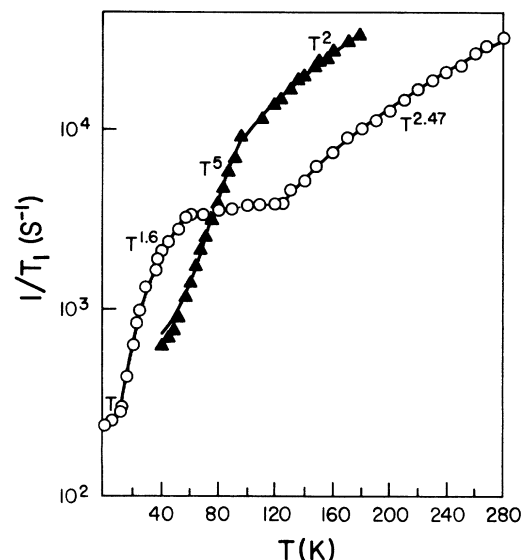


FIG. 4. $1/T_1$ vs temperature plot for ADA and RADA, with solid triangles for ADA and open circles for RADA.

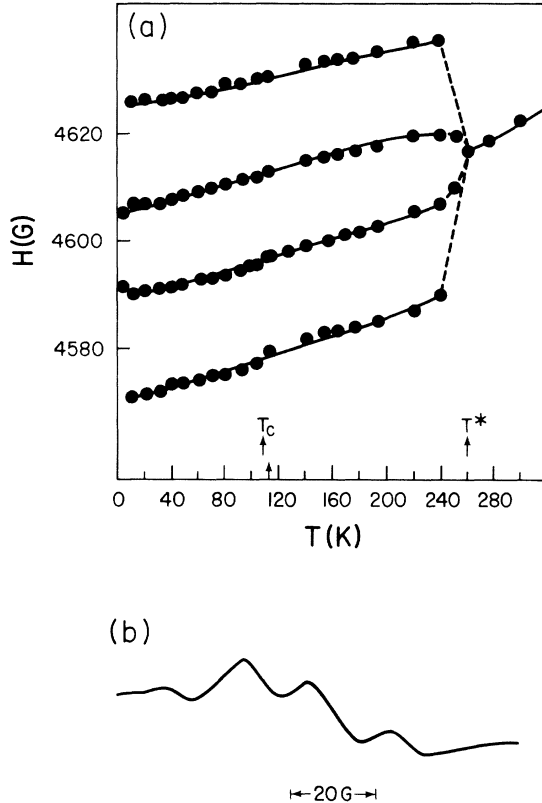


FIG. 5. (a) Line position evolution for AsO_4^{4-} center in RDA; (b) resolved spectra below T^* .

AsO_4^{4-} with different proton correlation times in mixed RADA. This leads us to expect different relaxation-time behavior in ADA compared to RADA. The temperature dependence of the normalized line intensities for AsO_4^{4-} and NH_3^+ ($m_N = \pm 1$) is presented in Fig. 6.

From Fig. 6, the direct coupling between AsO_4^{4-} and NH_3^+ spin levels is evident and is observed only in mixed RADA. The details of NH_3^+ motion in RADA and ADA are being presented by us in a separate paper,¹⁵ where a pronounced nitrogen tunneling motion was ob-

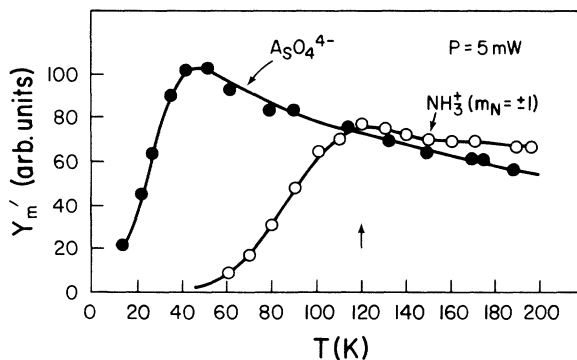


FIG. 6. The temperature dependence of normalized line intensities of AsO_4^{4-} and NH_3^+ centers in RADA ($P = 5$ mW).

served in RADA but not in ADA where, instead, the slowing down of protons of the NH_3^+ group leading to proton line splitting below about 115 K was observed. The nitrogen tunneling in NH_3^+ groups in RADA is evident in the temperature dependence of the line-intensity ratio between the $m_N = \pm 1$ nitrogen line and the $m_N = 0$ proton line.¹⁵ Vanishing of the $m_N = \pm 1$ line with decreasing temperature is the result of quadrupolar interaction between arsenic and nitrogen.

The ratio of hydrogen to nitrogen line intensity versus temperature allows us to determine the torsional energy $\hbar\omega_E$. The approximation for the tunneling frequency ω_t between the two lowest vibrational states has been given by Nanayanamutri and Pohl²⁸ as

$$\omega_t = 2\omega_E \left[\frac{2V_0}{\hbar\omega_E} \right]^{1/2} \exp \left[-\frac{2V_0}{\hbar\omega_E} \right], \quad (10)$$

with $\hbar\omega_E \ll V_0$, where V_0 is the tunneling barrier height. For $\hbar\omega_E = 0.035$ eV and $V_0 = 0.151$ eV,¹⁵ the tunneling frequency is of the order of the Larmor frequency ($\omega_{\text{EPR}} = 5.8 \times 10^{10} \text{ s}^{-1}$). Because of the sensitivity of Eq. (10) to the barrier height, in our case of random distribution of V_0 we can expect that ω_t is smeared out. This in turn leads to tunneling-assisted relaxation because of the quadrupole interaction of As with N. Stejskal and Gutowsky,²⁹ using Mathieu equations, show that the average tunneling frequency for various barrier heights V_0 flattens in the temperature region below about 100 K. Clough³⁰ discusses the distribution of tunneling frequency in samples with different barrier heights. The NMR data description of Lalowicz³¹ also shows that the influence of tunneling on T_1 is well established.

V. DISCUSSION AND CONCLUSIONS

The $1/T_1$ spin-lattice-relaxation curves presented in Fig. 4 were fit by several spin-relaxation models including the stretched exponential law used by Sobol *et al.*¹⁰ to explain the ⁸⁷Rb NMR T_1 anomaly in mixed crystals. No one model leads to a reasonable curve description over the whole temperature range. Recently, Wheeler *et al.*³² measured the relaxation time T_1 for $\text{KH}_2\text{PO}_4 \cdot \text{SeO}_4^{3-}$ doped crystals, and obtained the same order of T_1 as our values for ADA. They described the $1/T_1$ temperature dependence as the combination of direct and Raman process in a wide temperature range of 28–190 K. Cevc and Schara³³ found the relaxation rate of the AsO_4^{4-} center in ADA varies as $1/T_1 \propto T^{2.5}$ in the high- T region. The direct relaxation process seems unlikely to be important in the high-temperature region. We have observed $1/T_1 \propto T$ dependence in glassy RADA, but only below 12 K.

The relaxation curve for ADA diverges from $1/T_1 \propto T^2$ below 115 K where we observed¹⁵ the splitting of individual proton lines of NH_3^+ . So, below about 115 K the motion of acid protons in $\text{O}-\text{H} \cdots \text{O}$ bonds and NH_3^+ protons seem to be correlated. In this temperature region $1/T_1$ follows the law

$$1/T_1 = 10^{-6} T^5 + 1/T_{21}, \quad (11)$$

with $1/T_{21} = 6.65 \times 10^2 \text{ s}^{-1}$ as the temperature independent cross-relaxation time.³⁴ The T^5 relaxation dependence is characteristic of the Orbach-Blume process³⁵ (ground multiplet). Above 115 K the $1/T_1 \propto T^2$ two-phonon mechanism dependence was observed.

We will describe the RADA $1/T_1$ curve beginning from the lowest temperature. Below 12 K, $1/T_1 = AT$ as for the direct process. From 12 to 55 K, the relaxation seems to best fit $1/T_1 = 5.4T^{1.6}$. In the region 55 to 120 K, as we explained above, the relaxation process is driven by nitrogen tunneling. Above 120 K we again see the interesting behavior $1/T_1 = 2.7 \times 10^{-2} T^{2.47}$. There arises the question of the physical origin of such a temperature dependence.

It is known that a wide class of relaxation phenomena in disordered solids and glasses are nonexponential in time. In many cases, over a wide range of time the relaxation obeys a Kohlrausch-type³⁶ decay of the form $\phi(t) \sim \exp(-t/\tau)^\beta$. Randeria, Sethna, and Palmer³⁷ show, however, that exponential relaxation ($\beta=1$) above the spin-glass transition is ruled out because unfrustrated clusters do not dominate relaxation. It is also known that localized paramagnetic centers relax toward equilibrium (T_1 spin lattice relaxation) by inelastic scattering of lattice vibrations. Although the theory of relaxation is developed for phonons, an equivalent development has recently been accomplished for fractons.³⁷⁻⁴¹ This fracton theory was motivated by Stapleton's claim that EPR relaxation in proteins is governed by a fractal protein structure.⁴² The fractons are localized lattice vibrations³⁸ at distances less than some characteristic length L . It has been shown^{38,39} that, contrary to the single electronic relaxation-time constant obtained for extended vibrational states, vibrational localization leads to a probability density of relaxation-time constants with much richer temperature dependence.³⁹

The two-fracton Raman-type relaxation process for non-Kramers ions has the following temperature dependence:³⁹

$$1/T_1 \propto T^{2\bar{d}(1+2d_{\min}/\bar{d})-3}, \quad (12)$$

where \bar{d} is the fracton dimensionality, \bar{d} is the fractal network dimensionality, $d_{\min} = l/L$, l is the minimum distance traveled along the fractal network, and L is the Pythagorean length.⁴⁰ For a Euclidean lattice $\bar{d} = \bar{d} = d$ (d is the lattice dimensionality), $d_{\min} = 1$, and Eq. (12)

leads to the classical Raman process with $1/T_1 \propto T^7$. As has been shown by Orbach,⁴⁰ d_{\min} for a percolating network is 1.39 ($d_{\min} = 1$ holds for the Euclidean limit).

Now we can apply the above considerations to describe the EPR data for $1/T_1 \propto T^n$ with $n = 1.6$ and 2.47 in glassy RADA (Fig. 4). We found $1/T_1 \propto T^{1.6}$ in the temperature region of 12 to 55 K, and we can consider this region (below T_g) as the percolation limit where $\bar{d} = \frac{4}{3}$ holds.⁴¹ Then Eq. (12) leads to $\bar{d} = 3.83$ and $\bar{d}/\bar{d} = \beta \approx 0.35$, i.e., close to $\frac{1}{3}$ as obtained by Campbell⁴³ for random walks on closed loops in the percolation limit.

The physical origin of $1/T_1 \propto T^{2.47}$ above T_g is more speculative because all scaling corrections (d_{\min}, \bar{d}) have been done for the percolation limit (below T_g). Suppose, however, that above T_g we are dealing with a self-avoiding random walk in three-dimensional space, for which \bar{d} (fractal dimensionality) is equal⁴⁴ to 1.67; then for $d_{\min} \rightarrow 1$ Eq. (12) leads to $\bar{d} = 1.25$ and $\beta = 0.74$. This means that above T_g we have unpercolated fractons and the $1/T_1$ temperature dependence arises from fracton-phonon interaction.⁴⁰ The β value above T_g is then $\beta < 1$, and leads to nonexponentiality.³⁷

The most striking observation in the temperature region from 12 to 55 K is that the $1/T_1$ temperature dependence can be also described by the semiempirical Vogel-Fulcher (VF) law $1/T_1 = B(T - T_0)$ with $B = 82.5$ and with $T_0 = 12$ K as the VF freezing temperature. This indicates a temperature-independent energy distribution $f(U)$. Similarly, Slak *et al.*⁹ observed such behavior in ^{87}Rb T_1 relaxation measurements and suggested that it is due to random blocking of $\text{O}-\text{H} \cdots \text{O}$ acid proton movement.

In conclusion, EPR data indicate dynamical coupling between AsO_4^{4-} and NH_3^+ units which manifests itself in energy transfer from AsO_4^{4-} to NH_3^+ by tunneling coupling with $\omega_i \approx \omega_L$ (X band) (at 55 to 120 K). We have also shown that glassy-state relaxation rates can be described by the fracton model of relaxation. To our knowledge our EPR data give the first support for a fracton model of relaxation for mixed glassy RADA.

ACKNOWLEDGMENTS

This work was supported by National Science Foundation Grant Nos. DMR-8702933 and DMR-8714487.

*Permanent address: Institute of Molecular Physics, Polish Academy of Sciences, Poznan, Poland.

¹E. Courtens, *Ferroelectrics* **72**, 229 (1987).

²H. J. Bruckner, E. Courtens, and H. G. Unruh, *Z. Phys. B* **73**, 337 (1988).

³S. Hayase, T. Futumara, H. Sakashita, and H. Terauchi, *J. Phys. Soc. Jpn.* **54**, 812 (1985).

⁴R. Blinc, J. Dolinšek, R. Pirc, B. Tadić, and B. Zalar, *Phys. Rev. Lett.* **63**, 2248 (1989).

⁵V. H. Schmidt, *Ferroelectrics* **72**, 157 (1987).

⁶E. Courtens, T. F. Rosenbaum, S. E. Nagler, and P. M. Horn, *Phys. Rev. B* **29**, 515 (1984).

⁷Z. Trybula, V. H. Schmidt, J. E. Drumheller, D. He, and Z. Li, *Phys. Rev. B* **40**, 5289 (1989).

⁸R. Blinc, D. C. Ailion, B. Günther, and S. Zumer, *Phys. Rev. Lett.* **57**, 2826 (1986).

⁹J. Slak, R. Kind, R. Blinc, and S. Žumer, *Phys. Rev. B* **30**, 85 (1984).

¹⁰W. T. Sobol, I. G. Cameron, M. M. Pintar, and R. Blinc, *Phys. Rev. B* **35**, 7299 (1987).

- ¹¹V. H. Schmidt, J. T. Wang, and P. Schnackenberg, *Jpn. J. Appl. Phys.* **24**, Suppl. 2, 994 (1985).
- ¹²E. Courtens and H. Vogt, *Z. Phys. B* **62**, 143 (1986).
- ¹³E. Courtens, R. Vacher, and Y. Dagorn, *Phys. Rev. B* **33**, 7625 (1986).
- ¹⁴K. Parlinski and H. Grimm, *Phys. Rev. B* **32**, 1925 (1988).
- ¹⁵S. Waplak, Z. Trybula, J. E. Drumheller, and V. H. Schmidt (unpublished).
- ¹⁶M. Hampton, F. G. Herring, W. C. Lin, and C. A. McDowell, *Mol. Phys.* **10**, 565 (1966).
- ¹⁷N. S. Dalal, J. R. Dickinson, and C. A. McDowell, *J. Chem. Phys.* **57**, 4254 (1972).
- ¹⁸B. Lamotte, J. Gaillard, and O. Constantinescu, *J. Chem. Phys.* **57**, 3319 (1972).
- ¹⁹C. P. Poole, Jr., *Electron Spin Resonance* (Interscience, New York, 1967).
- ²⁰J. P. Lloyd and G. E. Pake, *Phys. Rev.* **94**, 579 (1954).
- ²¹M. J. Stephen and G. K. Frankel, *J. Chem. Phys.* **32**, 1435 (1960).
- ²²N. Bloembergen, E. M. Purcell, and R. V. Pound, *Phys. Rev.* **73**, 679 (1948).
- ²³A. M. Portis, *Phys. Rev.* **91**, 1071 (1953).
- ²⁴Varian Instrument Division (Models E-109, E-112, E-115).
- ²⁵R. Blinc, in *Proceedings of the Tenth Ampère Summer School, Portorož*, edited by R. Blinc, M. Vilfan, and J. Slak (J. Stefan Institute, Ljubljana, 1988), p. 143.
- ²⁶J. E. Wertz and J. Bolton, *Electron Spin Resonance* (McGraw-Hill, New York, 1972).
- ²⁷B. Ravkin and N. S. Dalal, *Phys. Rev. B* **39**, 7009 (1989).
- ²⁸V. Nanayanamurti and R. O. Pohl, *Rev. Mod. Phys.* **42**, 201 (1970).
- ²⁹E. O. Stejskal and H. S. Gutowsky, *J. Chem. Phys.* **28**, 388 (1958).
- ³⁰S. Clough, *J. Phys. C* **4**, 2180 (1971).
- ³¹Z. T. Lalowicz, *J. Phys. C* **16**, 2363 (1983).
- ³²E. D. Wheeler, H. A. Farach, C. P. Poole, Jr., and R. J. Creswick, *Phys. Rev. B* **37**, 9703 (1988).
- ³³P. Cevc and M. Schara, *Ferroelectrics* **7**, 113 (1976).
- ³⁴G. H. Larson and C. D. Jeffries, *Phys. Rev.* **145**, 311 (1966).
- ³⁵A. Abragam and B. Bleaney, *Electron Paramagnetic Resonance* (Clarendon, Oxford, 1970), and references therein.
- ³⁶C. Borczykowski and T. Kirski, *Phys. Rev. B* **40**, 11335 (1989).
- ³⁷M. Randeria, J. P. Sethna, and R. G. Palmer, *Phys. Rev. Lett.* **54**, 1324 (1985).
- ³⁸S. Alexander, O. Entin-Wohlman, and R. Orbach, *J. Phys. (Paris) Lett.* **46**, L-549 (1985).
- ³⁹S. Alexander, O. Entin-Wohlman, and R. Orbach, *J. Phys. (Paris) Lett.* **46**, L-555 (1985).
- ⁴⁰R. Orbach, *Science* **231**, 814 (1986), and references therein.
- ⁴¹S. Alexander and R. Orbach, *J. Phys. (Paris) Lett.* **43**, L-625 (1982).
- ⁴²H. J. Stapleton, J. P. Allen, C. P. Flynn, D. G. Stinson, and S. R. Kurtz, *Phys. Rev. Lett.* **45**, 1456 (1980).
- ⁴³I. A. Campbell, *J. Phys. (Paris) Lett.* **46**, L-1159 (1985).
- ⁴⁴B. B. Mandelbrot, *The Fractal Geometry of Nature* (Freeman, New York, 1983).